RESEARCH ARTICLE OPEN ACCESS

Glymphatic System May Mediate the Relation Between Choroid Plexus and Brain Damage in Multiple Sclerosis

Paolo Preziosa,[1,2,3] Elisabetta Pagani,[1] Monica Margoni,[1,2,4] Martina Rubin,[1,2,3] Loredana Storelli,[1] Gianluca Corazzolla,[1,3] Maria A. Rocca,[1,2,3] and Massimo Filippi[1,2,3,4,5]

Correspondence
Prof. Filippi
filippi.massimo@hsr.it

Neurol Neuroimmunol Neuroinflamm 2025;12:e200414. doi:10.1212/NXI.0000000000200414

Abstract

Background and Objectives

The choroid plexus (CP) regulates immune functions and produces most CSF that circulates in the brain parenchyma through perivascular spaces, part of the glymphatic system. In multiple sclerosis (MS), CP enlargement and glymphatic dysfunction are associated with inflammatory activity, clinical disability, and brain damage, but their interrelation is unclear. We investigated whether glymphatic system dysfunction mediates the association between CP enlargement and brain damage in patients with MS.

Methods

Brain fluid-attenuated inversion recovery, 3-dimensional T1-weighted, diffusion-weighted, and susceptibility-weighted sequences were obtained from 146 patients with MS and 72 healthy controls (HC). Glymphatic function was assessed using the diffusion along the perivascular space (DTI-ALPS) index, and CP volume was measured automatically.

Results

Patients with MS showed significantly higher white matter (WM) lesion and CP volumes ($p < 0.001$), and lower DTI-ALPS index, brain, WM, thalamic, and cortical volumes than HC ($p \leq 0.048$). In patients with MS, higher CP volume correlated with a lower DTI-ALPS index ($r = -0.305$, false discovery rate p value = 0.001). Both measures were associated with higher total, periventricular, and juxtacortical (JC) WM lesion volumes (CP volume: r from 0.285 to 0.340, p-FDR ≤ 0.001; DTI-ALPS index: r from −0.301 to −0.444, $p \leq 0.001$), and lower brain, thalamic, cortical, and WM volumes (CP volume: r from −0.246 to −0.405, p-FDR ≤ 0.006; DTI-ALPS index: from 0.269 to 0.497, p-FDR ≤ 0.003). The DTI-ALPS index partially mediated the associations of normalized choroid plexus volume with total, periventricular, and JC T2-hyperintense WM lesion volumes (standardized-β ranging from 0.073 to 0.115, relative effect ranging from 25.2% to 33.6%) and normalized brain, thalamic, cortical, and WM volumes (standardized-β ranging from −0.086 to −0.125, relative effect ranging from 25.3% to 52.7%).

Discussion

In MS, enlarged normalized CP volume may contribute to brain damage accumulation possibly through the promotion of a chronic proinflammatory state and the mediation of glymphatic system dysfunction.

Introduction

Multiple sclerosis (MS) is a chronic dysimmune disease of CNS characterized by inflammation, demyelination, and neurodegeneration.[1] Recent evidence suggested the choroid plexus (CP) as a potential contributor to MS pathophysiology.[2-11] The CP, a vascularized structure within the

[1]Neuroimaging Research Unit, Division of Neuroscience, IRCCS San Raffaele Scientific Institute, Milan, Italy; [2]Neurology Unit, IRCCS San Raffaele Scientific Institute, Milan, Italy; [3]Vita-Salute San Raffaele University, Milan, Italy; [4]Neurorehabilitation Unit, IRCCS San Raffaele Scientific Institute, Milan, Italy; and [5]Neurophysiology Service, IRCCS San Raffaele Scientific Institute, Milan, Italy.

The Article Processing Charge was funded by the authors.

This is an open access article distributed under the terms of the Creative Commons Attribution-Non Commercial-No Derivatives License 4.0 (CCBY-NC-ND), where it is permissible to download and share the work provided it is properly cited. The work cannot be changed in any way or used commercially without permission from the journal.

Copyright © 2025 The Author(s). Published by Wolters Kluwer Health, Inc. on behalf of the American Academy of Neurology.

Downloaded from https://www.neurology.org by San Raffaele - MI on 11 June 2025

Glossary

CP = choroid plexus; **DMT** = disease-modifying treatment; **DTI-ALPS** = diffusion along the perivascular space; **EDSS** = Expanded Disability Status Scale; **EM** = estimated mean; **ETL** = echo train length; **FA** = fractional anisotropy; **FDR** = false discovery rate; **FLAIR** = fluid-attenuated inversion recovery; **FOV** = field of view; **GM** = gray matter; **GMM** = Gaussian mixture model; **HC** = healthy control; **IT** = infratentorial; **JC** = juxtacortical; **LV** = lesion volume; **MS** = multiple sclerosis; **NBV** = normalized brain volume; **p-FDR** = false discovery rate p value; **ROI** = regions of interest; **SE** = standard error; **SWI** = susceptibility-weighted imaging; **TE** = echo time; **TR** = repetition time; **WM** = white matter.

cerebral ventricles, consists of a tight epithelial layer separated from fenestrated capillary endothelium by a cellular stroma.[2,10-14] It produces CSF and serves as an interface between the systemic immune system and the CNS.[2,10-14] Recent MRI studies have consistently shown a significant CP enlargement from the earliest phases of MS,[3-7] being associated with higher inflammatory activity,[3-7] more severe brain atrophy, clinical disability, and cognitive impairment.[3-7] Experimental models[2,3] and pathologic studies[8-11,15] suggest that CP enlargement in patients with MS likely reflects dysregulated immune cell migration and activation, and the release of proinflammatory factors within the CNS.[9,10] Given that the CP produces approximately 65%–80% of the total CSF,[14,16] its dysfunction may alter CSF secretion, affecting brain fluid dynamics and glymphatic system function, a brain-wide waste clearance network.[17,18] In the glymphatic system, CSF enters the brain parenchyma through the perivascular space around arteries and then moves into the interstitial space through an astrocytic aquaporin 4-dependent process, removing interstitial fluid waste products.[17,18] The interstitial fluid then drains through perivenous spaces to the meninges and meningeal lymphatic vessels near major venous sinuses.[17,18] Recently, the diffusion tensor image analysis along the perivascular space DTI-ALPS index has been proposed as a noninvasive method to evaluate glymphatic system function in vivo.[19] Lower DTI-ALPS index values are reported in both pediatric[20] and adult[21,22] patients with MS compared with matched healthy controls (HC), particularly those with progressive phenotypes[21] or cognitive impairment,[20] and are associated with more severe clinical disability and brain damage.[20,21]

CP enlargement and glymphatic system abnormalities may be interrelated pathologic processes contributing to lesion accumulation and brain atrophy in MS and other CNS conditions. In cerebral small vessel disease, the DTI-ALPS index partially mediates the association of CP volume with white matter (WM) lesion volume (LV) and growth,[23] as well as with information processing speed performance.[24] In Alzheimer disease, DTI-ALPS mediates relationships between WM lesion burden, Aβ accumulation, and cognitive function.[25] In a small cohort of patients with MS, the DTI-ALPS index was also found to partially mediate the association of CP volume with brain volume loss.[22] However, the specific associations between CP volume, glymphatic dysfunction, lesion distribution in MS-specific areas, and regional brain volume loss remain unclear.

We hypothesized that CP enlargement in MS is associated with abnormal CSF production and the release of proinflammatory factors, which, partially through an impaired glymphatic system, contribute to brain damage.

By evaluating a large cohort of patients with MS, this study aims to investigate whether impaired glymphatic function contributes to the observed relationships of CP enlargement with global and regional focal WM lesions and brain volumes.

Methods

Study Approval, Registration, and Patient Consents

The study was approved by the institutional ethics committee of IRCCS Ospedale San Raffaele (Protocol No. 2015–33). Written informed consent was obtained from all participants before study participation according to the Declaration of Helsinki.

Study Population

We retrospectively selected 146 consecutive patients with MS and 72 HC from the Neuroimaging Research Unit database at IRCCS San Raffaele Scientific Institute (Milan, Italy). All participants underwent the same MRI protocol between January 2019 and August 2022. Inclusion criteria for patients with MS were: age 18 years or older; a diagnosis of MS according to the 2017 revised McDonald criteria[26]; relapse-free and steroid-free for ≥3 months before MRI; no significant neurologic (other than MS), psychiatric, or systemic conditions; and stable MS treatment for ≥6 months. HC had no neurologic/systemic disorders affecting the CNS, and a normal neurologic examination.

Neurologic Assessment

Within 3 days from MRI acquisition, an experienced neurologist blinded to MRI findings assessed each patient, rating the Expanded Disability Status Scale (EDSS), determining MS phenotype (relapsing-remitting [RR] or progressive [P]), and recording disease-modifying treatment (DMT) status.

MRI Acquisition

Brain MRI was performed using a 3.0T Philips Ingenia CX scanner (Philips Medical Systems, receiving coil = dS-Head-32) between 1 PM and 8 PM to minimize sleep-related variability. Acquired sequences included (a) sagittal 3-dimensional (3D)

Downloaded from https://www.neurology.org by San Raffaele - MI on 11 June 2025

fluid-attenuated inversion recovery (FLAIR), field of view (FOV) = 256 × 256 mm, voxel size = 1 × 1 × 1 mm, 192 slices, matrix = 256 × 256, repetition time (TR) = 4,800 milliseconds, echo time (TE) = 270 milliseconds, inversion time (TI) = 1,650 milliseconds, echo train length (ETL) = 167, acquisition time = 6.15 minutes; (b) sagittal 3D T1-weighted turbo field echo, FOV = 256 × 256, voxel size = 1 × 1 × 1 mm, 204 slices, matrix = 256 × 256, TR = 7 milliseconds, TE = 3.2 milliseconds, TI = 1,000 milliseconds, flip angle = 8°, acquisition time = 8.53 minutes; (c) axial pulsed-gradient spin echo single-shot diffusion-weighted echo planar imaging 3 shells at b-value = 700/1000/2,855 seconds/mm^2 along 6/30/60 noncollinear directions and 10 b = 0 volumes were acquired, FOV = 240 × 233 mm, voxel size = 2.14 × 2.69 mm, 56 slices, 2.3 mm-thick matrix = 112 × 85, TR = 5,900 ms, TE = 78 ms, and 3 additional b = 0 volumes with reversed polarity of gradients for distortion correction, acquisition time = 10 minutes; (d) 3D T2-weighted scan, FOV = 256 × 256 mm, pixel size = 1 × 1 mm, 192 axial slices with 1 mm slice thickness, TR = 2,500 milliseconds, TE = 330 milliseconds, ETL = 117, acquisition time = 3 minutes; (e) 3D susceptibility-weighted imaging (SWI), FOV = 230 x 230, pixel size = 0.60 × 0.60 mm, 135 slices, 2 mm-thick, matrix = 384 x 382, TR = 39 milliseconds, TEs = 5.5:6:35.5 milliseconds, flip angle = 17°, acquisition time = 6 minutes; both magnitude and phase images for each echo were saved.

For all scans, slices were positioned parallel to the inferoanterior and inferoposterior corpus callosum.

Conventional MRI Analysis

Brain T2-hyperintense WM lesions were identified using a fully automated approach with 3D FLAIR and 3D T1-weighted,[27] and then T2-hyperintense WM LV was obtained for each patient from their lesion masks, after a careful visual inspection (Figure 1A).

For the definition of lesion topography, we first identified each lesion using a routine in Matlab that labels connected components; then, we transformed the relevant masks obtained from FMRIB Software Library (FSL)-SIENAx software (cortical gray matter [GM], lateral ventricles, cerebellum, and brainstem) onto the space of lesion segmentation and identified infratentorial (IT) lesions (i.e., cerebellar and brainstem lesions); after the application of a 3 mm sphere kernel, we identified periventricular and juxtacortical (JC) lesions as those touching the corresponding dilated masks; all the other lesions were coded as deep WM. For each class, we counted the total volume of T2-hyperintense WM lesions assigned.

Normalized volumes of the brain, thalamus, cortical, WM, and ventricles were quantified using FSL-SIENAx software and FSL-FIRST on lesion-filled 3D T1-weighted images, with a scaling factor derived from FSL-SIENAx (Figure 1B). Lateral ventricle volumes were calculated by manually removing the third and fourth ventricles from the ventricular masks generated by FSL-SIENAx.

CP Segmentation and Volume Quantification

A fully automatic method for CP segmentation was developed in-house, building on brain tissues segmentation obtained from the FSL-SIENAX toolbox,[28] as previously described (Figure 1C).[7]

The lateral ventricle mask from the Montreal Neurological Institute's standard 152-brain template (MNI-152 atlas) was affinely registered to each participant's space and eroded using a 1 mm filter to maintain a conservative approach.[29] The coregistered lateral ventricle mask was then used to distinguish peripheral from ventricular CSF within the global CSF segmentation. To eliminate potential boundaries with image intensities similar to CP on FLAIR contrast, WM, GM, and T2-hyperintense WM lesion masks were subtracted from each participant's lateral ventricle mask. The resulting "cleaned" ventricle mask was then registered to FLAIR space, and the corresponding image intensities were extracted. Since CP appear hyperintense on FLAIR while CSF signal is suppressed, a Gaussian mixture model (GMM) with 2 Gaussian distributions was applied, using the expectation-maximization algorithm to classify the data.[30] Voxels corresponding to the Gaussian distribution with lower intensities (CSF) were discarded. To further refine segmentation, a mean image filtering technique was applied to the binary mask, enhancing the distinction between CP voxels and spurious boundary voxels. A second GMM, again with 2 Gaussian distributions, was then applied to the filtered mask, and any residual voxel clusters smaller than 3 mm were removed. The final CP segmentation mask was thus obtained. The algorithm has been implemented in Matlab (R2017a, Mathworks). All CP segmentations were visually inspected and eventually edited in case of inaccuracies. Third and fourth ventricle CP was excluded because of inconsistent visualization.[6] CP and lateral ventricle volumes were then multiplied by V scaling (derived from the SIENAx) to obtain normalized values.[5,6]

Processing of Diffusion-Weighted Sequence

Preprocessing of diffusion-weighted images involved correcting for off-resonance effects, eddy current induced distortions, slice-to-volume misalignments, global movements, and for handling outliers using the Eddy tool within FSL.[31] The diffusion tensor was then estimated through linear regression, using diffusion-weighted imaging data at b = 700 and b = 1,000 seconds/mm^2. Then, eigenvalues and eigenvectors were computed through diagonalization of the diffusion tensor matrix, and fractional anisotropy (FA) maps were derived.[32]

Processing of SWI Sequence

To visualize brain venous vessels, local B0 field change maps were derived from multiecho SWI using the software available at github.com/sunhongfu/QSM. Briefly, phase images were first unwrapped to eliminate discontinuities caused by the limited phase range, using the best path method.[33] Then, a magnitude-weighted least squares regression was applied to fit unwrapped phase images to the TE. Finally, to make small veins visible, global spatial variations in the main magnetic

Downloaded from https://www.neurology.org by San Raffaele - MI on 11 June 2025

Figure 1 Examples of WM Lesion, Brain Volumetric, and CP Segmentation and of DTI-ALPS Index Calculation

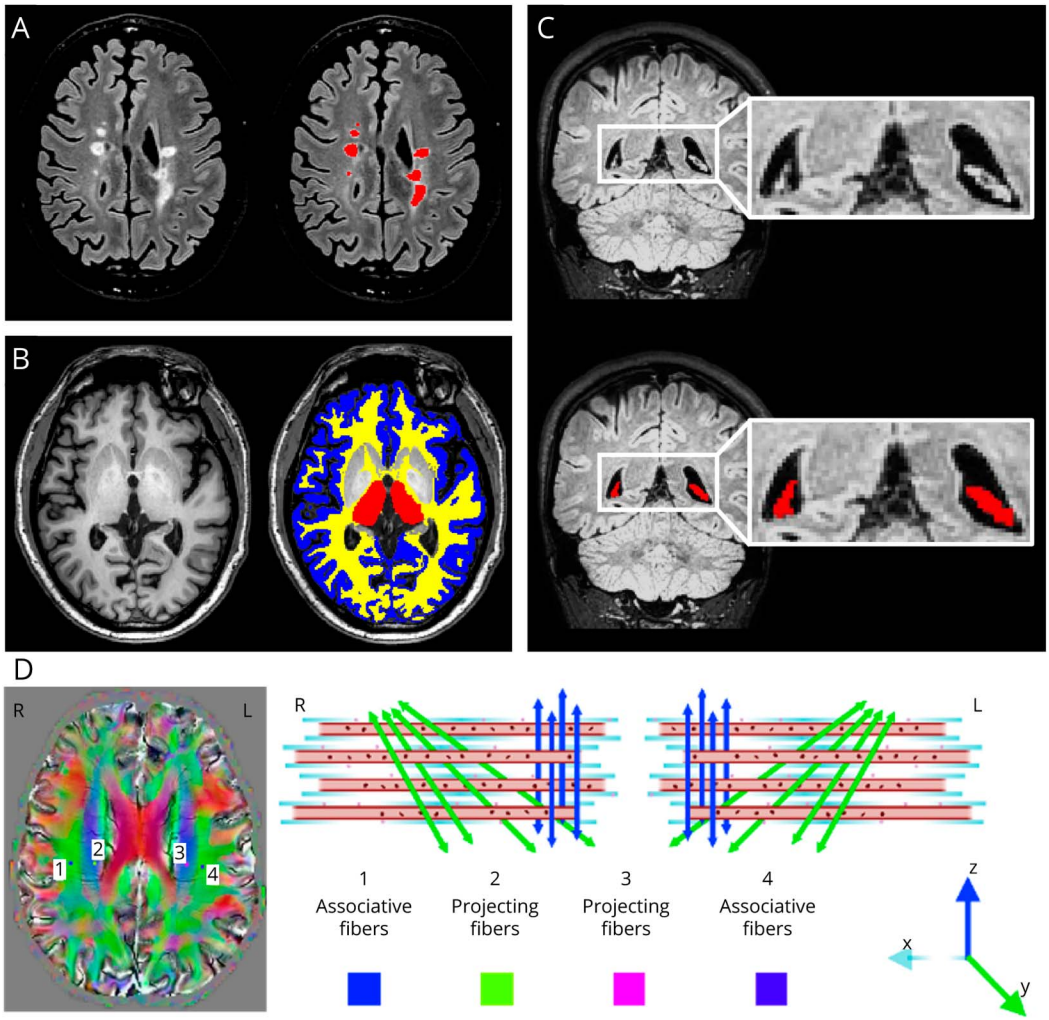

(A) Segmentation of brain T2-hyperintense WM lesions (red coded) on the 3D FLAIR sequence. (B) Segmentation of brain WM (yellow coded), cortex (blue coded), and thalamus (red coded) on 3D T1-weighted images using FSL-SIENAx software and FSL-FIRST tool. (C) CP segmentation (red coded) on the coronal plane of the 3D FLAIR sequence. (D) To calculate the DTI-ALPS index, the authors first registered the 3D FLAIR, the T2-hyperintense WM lesion mask and the FA map to the SWI scans. Three slices where veins run perpendicular to lateral ventricle were selected through SWI images. Over these slices, using the color-coded FA map in SWI space, four 3 × 3 × 3 mm regions of interest were drawn: 2 over the areas of associative fibers (see numbers 1 and 4), and the other 2 over the areas of projection fibers (see numbers 2 and 3) in the left and right hemispheres. Regions of interest were then registered to the diffusion space using the inverse of the FA map to the SWI registration matrix. Diffusivities along the *x*-, *y*-, and *z*-axes were extracted for each region of interest. DTI-ALPS was calculated as the ratio of diffusivities perpendicular to fiber bundles and parallel to veins (*Dx proj* and *Dx assoc*) over diffusivities perpendicular to fiber bundles and perpendicular to veins (*Dy proj* and *Dz assoc*). See text for further details. 3D = 3-dimensional; CP = choroid plexus; DTI-ALPS = diffusion tensor image analysis along the perivascular space; FA = fractional anisotropy; FLAIR = fluid attenuated inversion recovery; FSL = FMRIB Software Library; L = left; R = right; SWI = susceptibility-weighted imaging; WM = white matter.

field were removed using regularization enabled sophisticated harmonic artefact reduction for phase data.[34]

Quantification of DTI-ALPS Index

For each participant, the FA color map, the 3D FLAIR image, and the T2-hyperintense WM lesion mask were registered onto the SWI space using the magnitude of the first echo of the SWI sequence as a reference image. This image, which contains anatomical information, was aligned using rigid transformations, minimizing the normalized mutual information as cost function using FLIRT (FMRIB's Linear Image Registration Tool) in FSL (Figure 1D). The principal diffusion direction field images for each participant were then registered to the SWI images by applying the previously obtained rigid transformation matrix, using the "vecreg" utility from FSL.[35] All transformations were visually inspected to ensure proper coregistration.

Using the venous vessel map obtained from SWI images, we selected, for each participant, 3 contiguous axial slices where veins run perpendicular to the lateral ventricles to accurately define brain regions where veins, and thus perivascular spaces, are aligned along the *x*-axis.[19] Over these slices, color-coded principal diffusion direction maps were used to place 3 × 3 ×

Downloaded from https://www.neurology.org by San Raffaele - MI on 11 June 2025

3 mm cubic regions of interests (ROIs) at 2 sites per hemisphere: one ROI over projection fibers (*ROI proj*), where the major fiber axis corresponds to the *z*-axis, and the other ROI over associative fibers (*ROI assoc*), where the major fiber axis corresponds to the *y*-axis in the hemispheres. ROIs were drawn in both hemispheres to ensure robust data collection, reducing the effect of hemispheric dominance. In addition, the T2-hyperintense WM lesion mask was used to prevent ROI placement over visibly damaged tissue, ensuring that each ROI was positioned at least 2.5 mm in-plane from lesion edges. Once drawn, the ROIs were registered to the diffusion imaging space by applying the inverse diffusion-to-SWI transformation with linear interpolation. All voxels with values >0 were retained and visually inspected to ensure that only voxels corresponding to projection or associative fibers were included in *ROI proj* and *ROI assoc,* respectively. No further correction was applied. For each ROI, diffusivity along the x-, y-, and z-axes was extracted.

The DTI-ALPS was calculated as the ratio of diffusivities perpendicular to fiber bundles and parallel to veins (*Dx proj* and *Dx assoc*) over diffusivities perpendicular to fiber bundles and perpendicular to veins (*Dy proj* and *Dz assoc*).[19] This calculation leveraged the frame of reference established by the diffusion tensor eigenvectors and eigenvalues. We verified that secondary and tertiary eigenvectors were not affected by sorting bias issues.[36] The DTI-ALPS index was computed using the following formula:

$$DTI-ALPS\ index = \frac{mean(Dx\ proj, Dx\ assoc)}{mean(Dy\ proj, Dz\ assoc)}$$

The left and right hemisphere DTI-ALPS indices were averaged to obtain a mean DTI-ALPS index for each participant.

To evaluate DTI-ALPS index reproducibility, intraobserver and interobserver reliability was assessed by measuring the DTI-ALPS index in 15 randomly selected patients with MS, each evaluated twice by 2 independent raters (P.P. and M.M.) with a minimum interval of 15 days between assessments. Intraclass correlation coefficients were derived using a two-way random-effects model.

Statistical Analysis

Group differences of demographic and clinical variables between patients with MS and HC as well as between patients with progressive multiple sclerosis (PMS) and relapsing-remitting multiple sclerosis (RRMS) were tested using χ^2 tests, 2-sample *t* tests, or Mann-Whitney *U* tests, as appropriate. Between-group comparisons of brain lesional and volumetric measures and DTI-ALPS index were conducted using age-adjusted and sex-adjusted linear models. In the analysis of CP volume, normalized lateral ventricle volume and normalized brain volume (NBV) were included as additional covariates, as previously described.[6,7] T2-hyperintense WM LV was log-transformed.

Pairwise associations between CP volume, DTI-ALPS index, and structural MRI measures (including global and regional T2-hyperintense WM lesion volumes and global and regional brain volumes) were investigated in HC and patients with MS, separately, by age-adjusted and sex-adjusted partial correlations. These analyses were repeated with DMT status included as an additional covariate. In patients with MS, association with clinical variables (disease duration and EDSS score) was also investigated.

A mediation analysis was conducted to explore whether DTI-ALPS abnormalities, a proxy of glymphatic system integrity, acted as a mediator in the associations between CP volume and structural brain damage.

Mediation analyses were performed using PROCESS (version 4.2) for SPSS, adjusting for age and sex. The analysis was also repeated with DMT status included as an additional covariate. The simple mediation model (Model 4 in PROCESS) was used to test whether glymphatic function mediated the relationship between CP volume and structural brain damage.

For each relationship, regression coefficients and *p* values were obtained, quantifying the total, direct, and indirect effects of CP volume on structural brain damage. The bias-corrected and bias-accelerated bootstrap method (based on 5,000 replicates) was used to estimate a 95% CI for the indirect effect. In addition, the relative indirect and direct effects were calculated by taking the ratio of the corresponding regression coefficients to the total effect coefficient.

To control for multiple comparisons, the false discovery rate (FDR) correction was applied using the Benjamini-Hochberg procedure.

All statistical analyses were performed using SPSS software (version 26.0), with $p < 0.05$ considered statistically significant.

Data Availability

The corresponding author, who had full access to all study data, assumes responsibility for the integrity of the data and the accuracy of the analysis. The anonymized data set used and analyzed in this study is available on reasonable request from the corresponding author.

Results

Demographic, Clinical, and Conventional MRI Variables in Patients With MS Compared With HC

Table 1 summarizes the main demographic, clinical, and MRI features of HC and patients with MS.

Compared with HC, patients with MS had significantly higher T2-hyperintense WM LV ($p < 0.001$), as well as significantly

Downloaded from https://www.neurology.org by San Raffaele - MI on 11 June 2025

lower normalized brain ($p < 0.001$), thalamic ($p < 0.001$), cortical ($p = 0.048$), and WM volumes ($p < 0.001$), and enlarged lateral ventricle volume ($p < 0.001$) (Table 1).

Compared with RRMS, patients with PMS were significantly older ($p < 0.001$), had a longer disease duration ($p < 0.001$) and higher EDSS score ($p < 0.001$), and were more frequently untreated or treated with second-line DMTs ($p < 0.001$) (Table 1). Moreover, they had higher global and regional T2-hyperintense WM lesion volumes ($p < 0.001$) and lower global and regional brain volumes ($p \leq 0.041$), except for normalized WM volumes that were not significantly different between groups (Table 1).

CP Volume and Glymphatic System in Patients With MS

Compared with HC, patients with MS had significantly higher normalized CP volume (HC: estimated mean [EM] standard error [SE] = 2.52 mL [0.08]; patients with MS: EM [SE] = 3.00 [0.05], $p < 0.001$) (Table 1 and Figure 2A).

Manual DTI-ALPS index quantification showed a good reproducibility: the intraobserver reliability was 0.939 (95% CI = 0.830–0.979) and the interobserver reliability was 0.886 (95% CI = 0.682–0.967).

Table 1 Main Demographic, Clinical, and MRI Features of HC and Patients With MS

Variables	HC (n = 72)	MS (n = 146)	MS vs HC *p* value	RRMS (n = 103)	PMS (n = 43)	RRMS vs PMS *p* value
Sex (%): women/men	44 (61)/28 (39)	81 (56)/65 (45)	0.429[c]	59 (57)/44 (43)	22 (51)/21 (49)	0.498[c]
Mean age (SD) (y)	41.5 (12.6)	43.6 (11.2)	0.240[d]	41.0 (11.0)	49.9 (9.0)	<0.001[d]
Median disease duration (IQR) (y)	—	9.1 (1.9–19.7)	—	4.2 (1.1–15.8)	16.0 (8.3–23.0)	<0.001[g]
Median EDSS score (IQR)	—	2.0 (1.0–4.5)	—	1.5 (1.0–2.0)	6.5 (5.5–6.5)	<0.001[g]
Clinical phenotype (%): RRMS/PMS	—	103 (71)/43 (29)	—	—	14 (33)/29 (67)	—
Ongoing DMT (%)[a] none/ME/HE	—	17 (12)/79 (54)/50 (34)	—	6 (6)/71 (69)/26 (25)	11 (26)/8 (19)/24 (55)	<0.001[c]
Median total T2-hyperintense WM LV[b] (IQR) (mL)	0.00 (0.00; 0.19)	2.56 (0.90–7.85)	<0.001[e]	1.98 (0.73–4.41)	6.32 (2.76–13.12)	<0.001[e]
Median PV T2-hyperintense WM LV[b] (IQR) (mL)	—	1.70 (0.58–5.06)	-	1.19 (0.42–2.76)	5.72 (1.47–9.88)	<0.001[e]
Median JC T2-hyperintense WM LV[b] (IQR) (mL)	—	0.46 (0.99–1.25)	-	0.26 (0.06–1.11)	0.93 (0.42–1.44)	<0.001[e]
Median IT T2-hyperintense WM LV[b] (IQR) (mL)	—	0.06 (0.00–0.19)	-	0.02 (0.00–0.13)	0.18 (0.04–0.43)	<0.001[e]
Median deep WM T2-hyperintense WM LV[b] (IQR) (mL)	—	0.16 (0.09–0.30)	-	0.16 (0.08–0.29)	0.20 (0.10–0.31)	<0.001[e]
EM (SE)						
Normalized brain volume (mL) EM (SE)	1,553 (6)	1,518 (4)	<0.001[e]	1,525 (6)	1,494 (8)	0.002[e]
Normalized thalamic volume (mL) EM (SE)	22.0 (0.2)	20.3 (0.2)	<0.001[e]	20.7 (0.2)	19.3 (0.3)	<0.001[e]
Normalized cortical volume (mL) EM (SE)	652 (4)	643 (3)	0.048[e]	646 (3)	632 (6)	0.041[e]
Normalized WM volume (mL) EM (SE)	687 (4)	664 (3)	<0.001[e]	667 (3)	656 (3)	0.083[e]
Normalized choroid plexus volume (mL) EM (SE)	2.52 (0.08)	3.00 (0.05)	0.001[f]	3.07 (0.07)	3.14 (0.11)	0.574[f]
Normalized lateral ventricle volume (mL) EM (SE)	20.8 (1.7)	30.3 (1.2)	<0.001[e]	28.6 (1.6)	35.8 (2.5)	0.018[e]
DTI-ALPS index	1.695 (0.019)	1.597 (0.014)	<0.001[e]	1.596 (0.016)	1.598 (0.026)	0.957[e]

Abbreviations: DMT = disease-modifying therapy; DTI-ALPS = diffusion tensor image analysis along the perivascular space; EDSS = Expanded Disability Status Scale; EM = estimated mean; HC = healthy controls; HE = high efficacy; IQR = interquartile range; IT = infratentorial; JC = juxtacortical; LV = lesion volume; ME = moderate efficacy; mL = milliliter; MS = multiple sclerosis; NBV = normalized brain volume; P = progressive; PV = periventricular; RR = relapsing remitting; SE = standard error; WM = white matter.
DTI-ALPS is a dimensionless index.
[a] ME DMT = glatiramer acetate, interferon β-1a, teriflunomide or dimethyl fumarate; HE DMT = fingolimod, siponimod, natalizumab, cladribine, ocrelizumab, rituximab, alemtuzumab, other immunosuppressants.
[b] Comparison performed on log-scale.
[c] Chi-squared test.
[d] Two-sample *t* test.
[e] Age-adjusted and sex-adjusted linear regression model.
[f] Age-adjusted, sex-adjusted, normalized brain and lateral ventricle volume-adjusted linear regression model.
[g] Mann-Whitney *U* Test.

Downloaded from https://www.neurology.org by San Raffaele - MI on 11 June 2025

Compared with HC, patients with MS had also significantly lower DTI-ALPS index (HC: EM [SE] = 1.695 [0.019]; patients with MS: EM [SE] = 1.597 [0.014], $p < 0.001$) (Table 1 and Figure 2B).

Differences in normalized CP volume and DTI-ALPS index were not significant between patients with RRMS and PMS ($p \geq 0.574$) (Table 1).

Analysis of Correlation

In HC, normalized CP volume was not correlated with the DTI-ALPS index (false discovery rate p value [p-FDR] = 0.997) (Table 2). Moreover, both normalized CP volume and DTI-ALPS index showed no significant correlations with total T2-hyperintense WM LV, global and regional brain volumetric measure (p-FDRp ≥ 0.342), except for a significant correlation between higher DTI-ALPS index and higher normalized thalamic volume ($r = 0.288$, p-FDR = 0.030) (Table 2).

In patients with MS, a higher normalized CP volume was significantly correlated with a lower DTI-ALPS index ($r = -0.305$, p-FDR = 0.001) (Table 2, Figure 1C). A higher normalized CP volume was also significantly correlated with a longer disease duration ($r = 0.247$, p-FDR = 0.006), higher total, periventricular, and JC brain T2-hyperintense WM lesion volumes (r values ranging from 0.285 to 0.340, p-FDR ≤ 0.002), and lower normalized brain, thalamic, cortical, and WM volumes (r values ranging from −0.246 to −0.405, p-FDR ≤ 0.006) (Table 2, Figure 3). Normalized CP volume was not significantly correlated with EDSS score ($r = 0.181$, p-FDR = 0.054), IT, and deep WM T2-hyperintense WM lesion volumes (p-FDR ≥ 0.176).

In patients with MS, a lower DTI-ALPS index was significantly correlated with a longer disease duration ($r = -0.246$, p-FDR = 0.006), higher total, periventricular, and JC brain T2-hyperintense WM lesion volumes (r values ranging from −0.301 to −0.444, p-FDR ≤ 0.001), and lower normalized brain, thalamic, cortical, and WM volumes (r values ranging from 0.269 to 0.497, p-FDR ≤ 0.003) (Table 2, Figure 3). The DTI-ALPS index was not significantly correlated with EDSS, IT, and deep WM T2-hyperintense WM lesion volumes (p-FDR ≥ 0.342). Results did not change including DMT as an additional covariate (data not shown).

Mediation Models in Patients With MS

Higher CP volume was significantly associated with higher total (standardized β = 0.332, p-FDR < 0.001), periventricular (standardized β = 0.343, p-FDR < 0.001), and JC T2-hyperintense WM lesion volumes (standardized β = 0.291, p-FDR < 0.001), but not with higher IT or deep WM T2-hyperintense WM lesion volumes (Figure 4).

The DTI-ALPS index partially mediated the association between CP volume and total (indirect standardized β = 0.101, 95% CI = 0.042–0.169, mediated effect = 30.5%), periventricular (indirect standardized β = 0.115, 95% CI = 0.051–0.188, mediated effect = 33.6%), and JC brain T2-hyperintense WM lesion volumes (indirect standardized β = 0.073, 95% CI = 0.013–0.145, mediated effect = 25.2%) (Figure 4).

Higher CP volume was significantly associated with lower NBV (standardized β = −0.364, p-FDR < 0.001), normalized

Figure 2 Normalized Choroid Plexus Volume and DTI-ALPS Index Distributions in Patients With MS and HC and Partial Correlation Analyses Between Normalized Choroid Plexus Volume and DTI-ALPS Index in Patients With MS

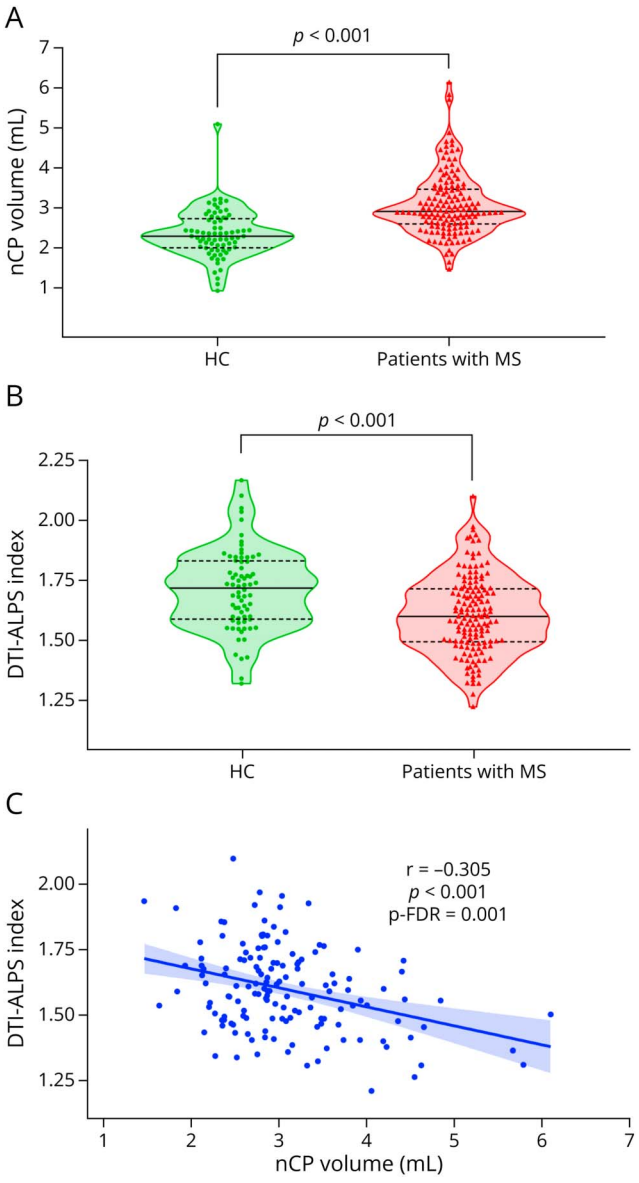

Violin plots showing the distribution of (A) normalized choroid plexus volume and (B) DTI-ALPS index in patients with MS and HC. (C) Age-adjusted and sex-adjusted partial correlations between normalized choroid plexus volume and DTI-ALPS index in patients with MS. See text for further details. DTI-ALPS = diffusion tensor image analysis along the perivascular space; HC = healthy controls; mL = milliliter; MS = multiple sclerosis; nCP = normalized choroid plexus.

Downloaded from https://www.neurology.org by San Raffaele - MI on 11 June 2025

Table 2 Age-Adjusted and Sex-Adjusted Partial Correlation Between Choroid Plexus Volume, DTI-ALPS Index, and Brain Structure Volume in Patients With MS and HC

	Normalized choroid plexus volume				DTI-ALPS index			
	HC		Patients with MS		HC		Patients with MS	
	r value	*p* Value (p-FDR)	*r* value	*p* Value (p-FDR)	*r* value	*p* Value (p-FDR)	*r* value	*p* Value (p-FDR)
Disease duration (y)	—	—	0.247	0.003 (0.006)	—	—	−0.246	0.003 (0.006)
EDSS score	—	—	0.181	0.030 (0.054)	—	—	0.029	0.726 (0.796)
Total T2-hyperintense WM LV[a] (mL)	−0.025	0.835 (0.867)	0.328	<0.001 (<0.001)	0.129	0.286 (0.389)	−0.397	<0.001 (<0.001)
PV T2-hyperintense WM LV[a] (mL)	—	—	0.340	<0.001 (<0.001)	—	—	−0.444	<0.001 (<0.001)
JC T2-hyperintense WM LV[a] (mL)	—	—	0.285	0.001 (0.002)	—	—	−0.301	<0.001 (0.001)
IT T2-hyperintense WM LV[a] (mL)	—	—	0.136	0.104 (0.176)	—	—	−0.103	0.221 (0.342)
Deep WM T2-hyperintense WM LV[a] (mL)	—	—	0.057	0.496 (0.646)	—	—	−0.040	0.637 (0.722)
Normalized brain volume (mL)	−0.135	0.266 (0.377)	−0.405	<0.001 (<0.001)	0.070	0.563 (0.660)	0.497	<0.001 (<0.001)
Normalized thalamic volume (mL)	−0.150	0.216 (0.342)	−0.246	0.003 (0.006)	0.288	0.016 (0.030)	0.461	<0.001 (<0.001)
Normalized cortical volume (mL)	−0.076	0.532 (0.646)	−0.327	<0.001 (<0.001)	0.078	0.523 (0.646)	0.346	<0.001 (<0.001)
Normalized WM volume (mL)	−0.135	0.266 (0.377)	−0.247	0.003 (0.006)	0.024	0.842 (0.867)	0.269	0.001 (0.003)
Normalized choroid plexus volume (mL)	—	—	—	—	−0.001	0.997 (0.997)	−0.305	<0.001 (0.001)
DTI-ALPS index	−0.001	0.997 (0.997)	−0.305	<0.001 (0.001)	—	—	—	—

Abbreviations: DTI-ALPS = diffusion tensor image analysis along the perivascular space; EDSS = Expanded Disability Status Scale; HC = healthy controls; IT = infratentorial; JC = juxtacortical; LV = lesion volume; mL = milliliter; MS = multiple sclerosis; p-FDR = =false discovery rate *p* value; PV = periventricular; WM = white matter.
DTI-ALPS is a dimensionless index.
[a] Analysis performed on log-scale.

thalamic volume (standardized β = −0.238, p-FDR = 0.004), normalized cortical volume (standardized β = −0.296, p-FDR < 0.001), and normalized WM volume (standardized β = −0.258, p-FDR = 0.004) (Figure 5).

The DTI-ALPS index partially mediated the association between CP volume and NBV (indirect standardized β = −0.113, 95% CI = −0.183 to −0.051, mediated effect = 31.0%), normalized thalamic volume (indirect standardized β = −0.125, 95% CI = −0.197 to −0.059, mediated effect = 52.7%), normalized cortical volume (indirect standardized β = −0.075, 95% CI = −0.133 to −0.027, mediated effect = 25.3%), normalized WM volume (indirect standardized β = −0.068, 95% CI = −0.130 to −0.014, mediated effect = 26.3%) (Figure 5).

Results did not change including DMT as an additional covariate (data not shown).

Discussion

This study found that patients with MS exhibited significantly larger CP volumes and lower DTI-ALPS index, a proposed marker of glymphatic system function, compared with HC. Both abnormalities were significantly associated with higher T2-hyperintense WM LV and brain volume loss. In patients with MS, the DTI-ALPS index partially mediated the relationship between CP enlargement and structural brain damage.

Consistent with previous studies,[3-7] we observed significant CP enlargement in patients with MS compared with HC, suggesting that CP abnormalities may play a role in disease pathology. It is important that CP enlargement was significantly associated with longer disease duration, and more extensive brain damage, including higher T2-hyperintense WM lesion volumes and lower global and regional brain volumes. Of interest, neither normalized CP volume nor DTI-ALPS index differed significantly between patients with RRMS and PMS, aligning with prior findings,[5,21] and suggesting that CP and glymphatic system abnormalities may represent an early phenomenon in the disease course.

The CP regulates CSF production and serves as an interface between the CNS and the peripheral immune system,[2,10-13] facilitating lymphocyte entry from peripheral blood into the CNS and acting as a CSF monitoring and antigen-presenting site.[2,10-13] In MS, the CP stroma and vessels show higher immune cell aggregates, increased expression of vascular adhesion molecules, and structural alterations such as abnormal capillary permeability, basement membrane thickening, and ependymal cell cilia loss.[10,11,37] In addition, hypoxia in the CP environment of patients with MS may impair CSF secretion and neuroprotective functions,[9] fostering a chronic and

Downloaded from https://www.neurology.org by San Raffaele - MI on 11 June 2025

Figure 3 Partial Correlation Analyses in Patients With MS

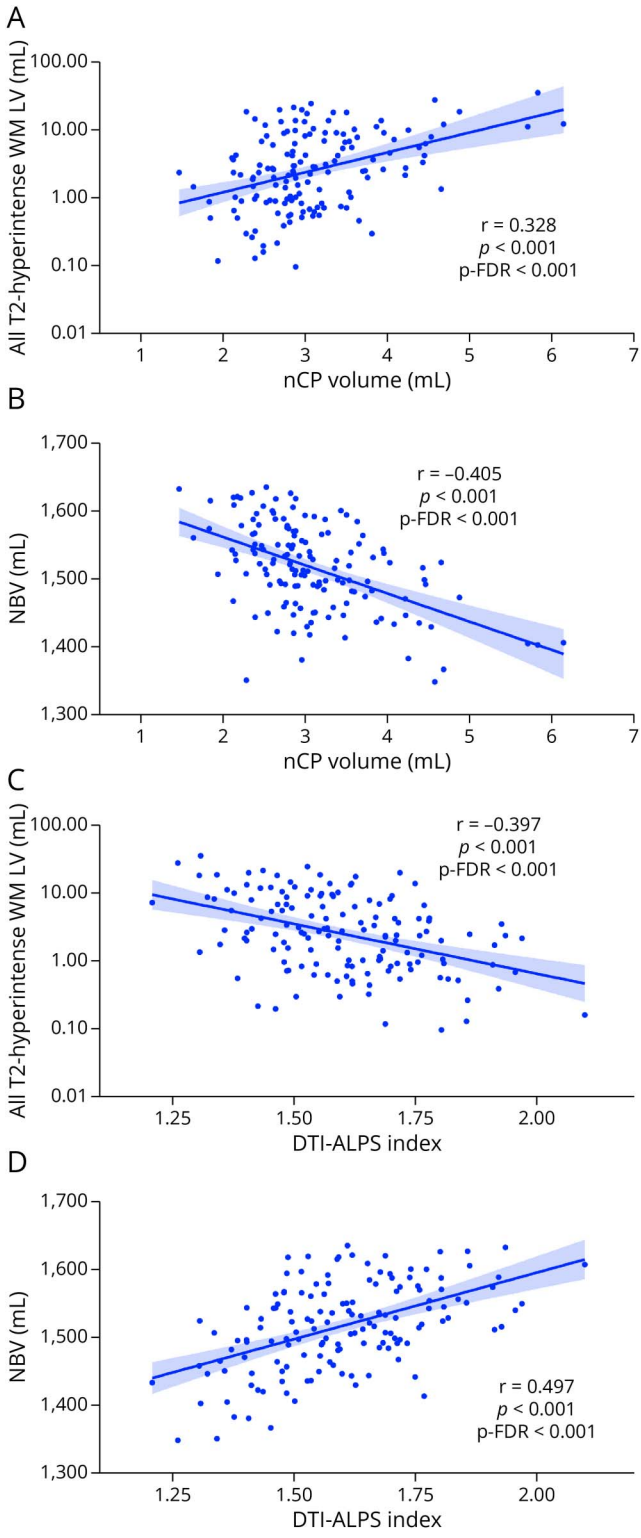

Age-adjusted and sex-adjusted partial correlations in patients with MS between (A) normalized choroid plexus volume and all T2-hyperintense WM lesion volume, (B) normalized choroid plexus volume and NBV, (C) DTI-ALPS index and all T2-hyperintense WM lesion volume, and (D) DTI-ALPS index and NBV. See text for further details. DTI-ALPS = diffusion tensor image analysis along the perivascular space; mL = milliliter; LV = lesion volume; NBV = normalized brain volume; nCP = normalized choroid plexus; p-FDR = false discovery rate *p* value; WM = white matter.

detrimental proinflammatory state in the CNS mediated by CSF. Supporting this hypothesis, and in line with previous studies,[3-7] we found that CP enlargement in patients with MS was significantly associated with greater focal demyelination, particularly in periventricular and JC areas. In addition, CP volume significantly correlated with global and regional brain volume loss, suggesting link between chronic inflammation, CP abnormalities, and neurodegeneration.

Notably, CP enlargement is not unique to MS,[3-7] but it is also observed in other neurodegenerative disorders, including cerebral small vessel disease,[23,24] and Alzheimer disease.[25,38] Although inflammatory processes may play a role in these conditions, they are typically more limited, suggesting that CP enlargement may also underlie other pathologic processes beyond inflammatory aggregates that are shared among different diseases. CP enlargement has been associated with reduced CP permeability,[38] and a lower rate of CSF secretion,[38] likely due to pathologic substrates underlying such an impaired CSF production; these may include CP fibrosis, with fibrous thickening of pericapillary membranes, increased immune cells and fibroblasts, and deposition of collagen, fibrinogen, and proteins like β-amyloid in Alzheimer disease.[39,40] These processes may determine a decreased CSF turnover,[39,40] prolonging the persistence of proinflammatory and toxic factors in the CSF, which could contribute to brain damage through glymphatic system dysfunction.

Supporting this hypothesis, our findings suggested a significant association between CP volume and DTI-ALPS index, a proposed measure of glymphatic system function, reinforcing the notion that these pathologic processes are interconnected. Similarly to previous studies,[20-22] we found that patients with MS had a significantly lower DTI-ALPS index compared with HC, suggesting a possible impaired glymphatic system function. Moreover, a lower DTI-ALPS index was significantly associated with longer disease duration, higher total, periventricular, and JC T2-hyperintense WM lesion volumes, as well as lower brain, thalamic, cortical, and WM volumes.

Consistently with previous studies on cerebral small vessel disease[24,41] and MS,[22] we also found that larger CP volume was significantly associated with a lower DTI-ALPS index.

Mediation analyses further indicated that the DTI-ALPS index partially mediates the relationship between CP enlargement and structural brain damage.[22] This supports the hypothesis that CP enlargement may contribute to focal WM lesions and irreversible tissue loss, at least partially, through impaired glymphatic clearance. A reduction in CSF secretion,[38] combined with immune cell accumulation, inflammatory factor retention, and impaired CSF-interstitial fluid exchange, may disrupt waste clearance, exacerbating neuroinflammation, and brain damage.

Downloaded from https://www.neurology.org by San Raffaele - MI on 11 June 2025

Figure 4 Partial Mediation Effect of DTI-ALPS Index Between Choroid Plexus Volume and T2-Hyperintense WM Lesion Volumes in Patients With MS

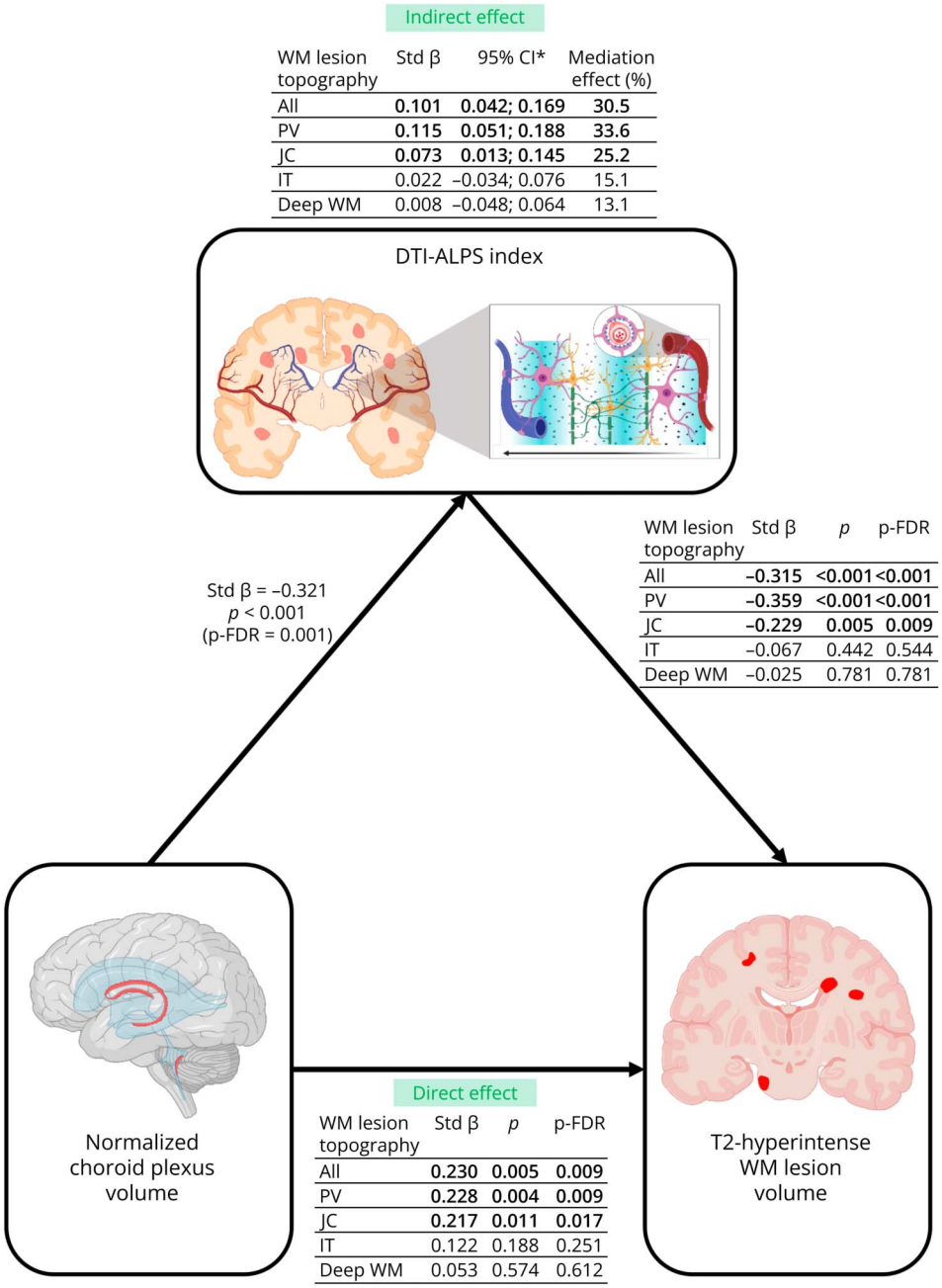

The DTI-ALPS index partially mediated the association between choroid plexus volume and all, PV and JC WM lesion volumes. Mediation analysis was adjusted for age and sex. Created in BioRender. Preziosa, P. (2025)//BioRender.com/w88vafq. *Bias corrected and accelerated bootstrapped CI based on 5,000 samples. PROCESS (version 4.2) for SPSS primarily uses bootstrap CI to assess the significance of indirect effects instead of relying on traditional *p* values. If the 95% CI does not contain zero, the indirect effect is considered significant. Accordingly, all the direct effect with the 95% CI does not contain zero should be considered statistically significant ($p < 0.05$). DTI-ALPS = diffusion tensor image analysis along the perivascular space; IT = infratentorial; JC = juxtacortical; LV = lesion volume; MS = multiple sclerosis; p-FDR = false discovery rate *p* value; PV = periventricular; std β = standardized β; WM = white matter.

As the glymphatic system is responsible for clearing up to 70% of interstitial solutes and proteins,[18] its dysfunction may lead to inefficient removal of toxic and proinflammatory factors, fostering a chronic, detrimental CNS environment. This mechanism could explain why glymphatic system impairment is observed not only in MS but also in aging,[42] and various neurologic disorders.[24,41,43] This hypothesis is also consistent with the evidence that a higher DTI-ALPS index was significantly associated with higher thalamic volume in HC. A more efficient glymphatic system may contribute to preserving thalamic volume, by preventing neurodegeneration and supporting cellular homeostasis. This may be particularly relevant for the thalamus considering its high interconnection with many brain regions and substantial energy demand.

However, the DTI-ALPS index only partially mediates the association between CP enlargement and brain damage, indicating that other CP-related pathologic processes independent of glymphatic dysfunction may also contribute to MS-related structural CNS damage. These processes include the CSF-in gradient of damage observed in patients with MS,[44] with focal demyelinating lesions and neuroaxonal loss

Downloaded from https://www.neurology.org by San Raffaele - MI on 11 June 2025

Figure 5 Partial Mediation Effect of DTI-ALPS Index Between Choroid Plexus Volume and Brain Volumes in Patients With MS

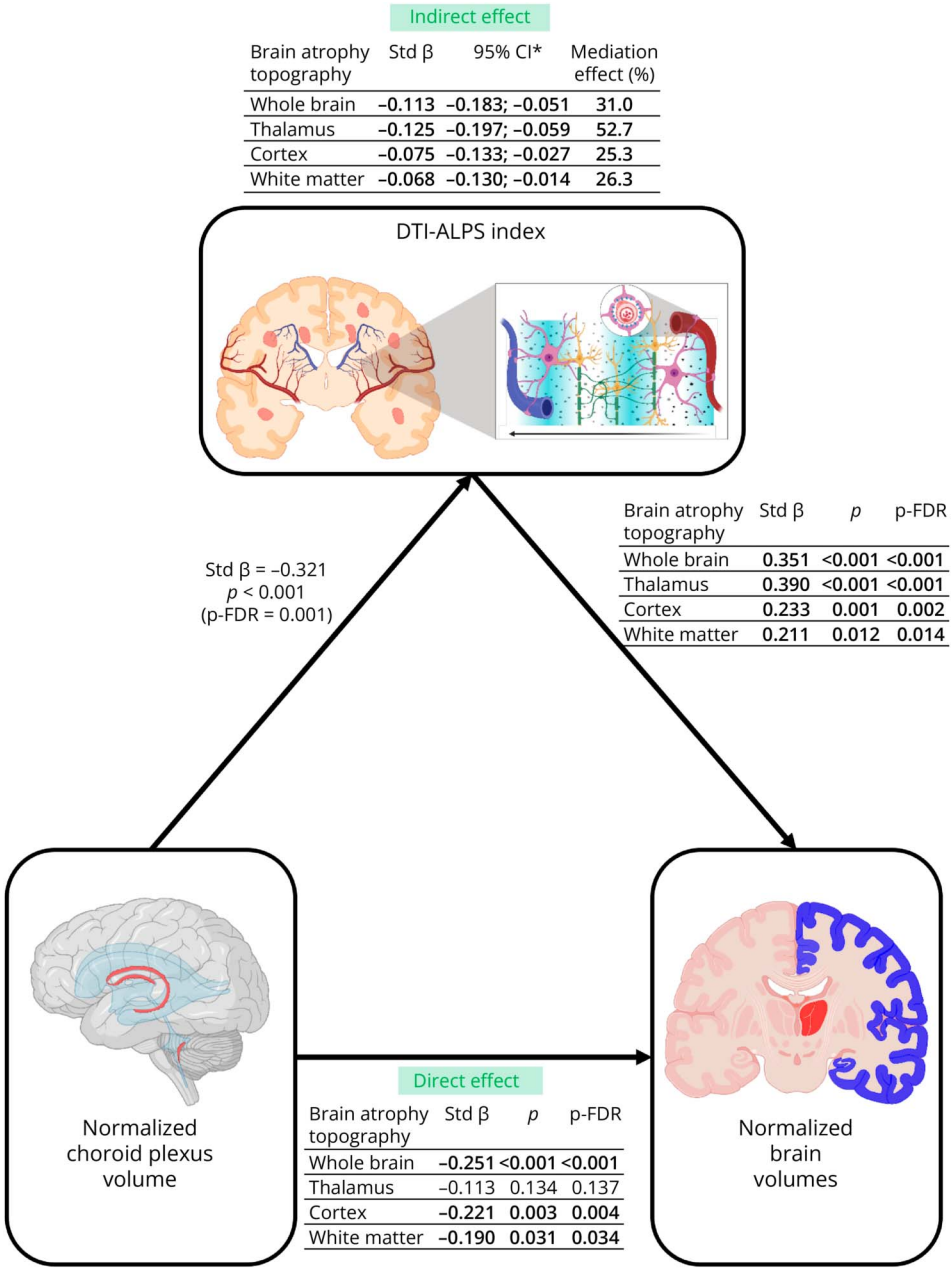

The DTI-ALPS index partially mediated the association between choroid plexus volume and normalized brain, thalamic, cortical, and WM volumes. Mediation analysis was adjusted for age and sex. Created in BioRender. Preziosa, P. (2025) BioRender.com/. *Bias corrected and accelerated bootstrapped CI based on 5,000 samples. PROCESS (version 4.2) for SPSS primarily uses bootstrap CI to assess the significance of indirect effects instead of relying on traditional *p* values. If the 95% CI does not contain zero, the indirect effect is considered significant. Accordingly, all the direct effect with the 95% CI does not contain zero should be considered statistically significant ($p < 0.05$). DTI-ALPS = diffusion tensor image analysis along the perivascular space; MS = multiple sclerosis; p-FDR = false discovery rate *p* value; std β = standardized β.

being more severe in periventricular areas, deep GM nuclei, and subpial cortical regions.[44]

Our study has several limitations, warranting cautious in interpreting the results. The cross-sectional design prevents analysis of longitudinal changes in CP volume, glymphatic function, and brain damage. Future longitudinal studies are needed to explore these dynamics over time. Although the DTI-ALPS index provides a noninvasive assessment of glymphatic function, it does not represent whole-brain glymphatic activity because it only reflects diffusivity in selected brain regions. Whole-brain glymphatic function is more complex, with perivascular space diffusion representing just 1 step in the waste clearance process. Therefore, a multiparametric study combining contrast-based dynamic approaches (i.e., MRI after intrathecal or IV gadolinium-based contrast agent administration) with the DTI-ALPS index may further elucidate the interplay among CP enlargement, glymphatic system dysfunction, and brain damage. Direct histopathologic validation of the DTI-ALPS index is currently lacking, and diffusion abnormalities in normal-appearing WM may reflect a combination of glymphatic dysfunction and other MS-related pathophysiologic processes, including inflammation, demyelination, axonal damage, and astrogliosis,

Downloaded from https://www.neurology.org by San Raffaele - MI on 11 June 2025

limiting the specificity of the DTI-ALPS index as a marker of glymphatic system function. However, a recent study has provided indirect evidence of the interplay between the CP and glymphatic dysfunction, as quantified by the DTI-ALPS index.[23] Using a 3D T1-weighted sequence acquired before and 39 hours after intrathecal gadolinium administration, the study found that patients with a larger CP volume exhibited impaired glymphatic clearance.[23] Moreover, in a separate longitudinal cohort, the DTI-ALPS index was shown to partially mediate the effect of CP enlargement on both WM lesion severity and progression.[23] Furthermore, glymphatic function is strongly regulated by sleep, but sleep data were not available in our cohort. To minimize confounding effects, MRI scans were conducted between 1 PM and 8 PM, but future studies should explore the role of sleep duration and quality in MS-related glymphatic dysfunction. The presence of T2-hyperintense WM lesions may have influenced ROI placement for DTI-ALPS analysis. However, the regions evaluated, including projection fibers (mainly the corticospinal tract) and association fibers (mainly the superior longitudinal fasciculus), are relatively large WM tracts spanning multiple slices, allowing for reliable ROI placement. Despite potential subjectivity, manual DTI-ALPS ROI placement remains the gold standard, having been widely validated and applied in previous studies.[19,21,22,25] Although atlas-based methods offer automation, they present limitations, including individual variability in WM anatomy and challenges in accurately capturing DTI-ALPS–specific regions, particularly in neurodegenerative and demyelinating disorders. A strength of our study is the integration of SWI, which enhances venous vessel visualization and improves ROI placement standardization. In addition, the high intrarater and interrater agreement supports the validity and accuracy of the current manual approach. The lack of association between CP volume and IT or deep WM T2-hyperintense lesion volumes may be partially due to the exclusion of third and fourth ventricle CP from the analysis. However, since CSF circulates throughout the CNS, this is unlikely to fully explain the findings. Deep WM lesion pathophysiology may differ from other regions. The relatively lower LV in these areas compared with periventricular and JC regions may have reduced the statistical power to detect significant associations. Finally, histopathologic studies have already suggested the presence of inflammatory infiltrates within the CP stroma, along with possible structural changes such as fibrosis.[9-11,15,39,40] These findings highlight the likelihood that specific genetic and immunologic factors may be relevant in driving CP enlargement in MS. However, these data were not available for our patients with MS. Future studies integrating advanced immunoprofiling, genetic analyses, and longitudinal follow-ups are warranted to unravel the underlying mechanisms and to determine whether CP volume changes are primarily an epiphenomenon of systemic CNS inflammation or a contributing factor to MS pathology itself.

In conclusion, in MS, enlarged CP may contribute to brain damage accumulation, partially through an impaired glymphatic system clearance. If confirmed in future studies, these processes, evaluable in vivo using MRI, could represent novel therapeutic targets for developing therapies for mitigating the detrimental effects of MS on brain damage and irreversible clinical disability.

Author Contributions

P. Preziosa: drafting/revision of the manuscript for content, including medical writing for content; major role in the acquisition of data; study concept or design; analysis or interpretation of data. E. Pagani: drafting/revision of the manuscript for content, including medical writing for content; major role in the acquisition of data; analysis or interpretation of data. M. Margoni: drafting/revision of the manuscript for content, including medical writing for content; major role in the acquisition of data; analysis or interpretation of data. M. Rubin: drafting/revision of the manuscript for content, including medical writing for content; major role in the acquisition of data; analysis or interpretation of data. L. Storelli: drafting/revision of the manuscript for content, including medical writing for content; analysis or interpretation of data. G. Corazzolla: drafting/revision of the manuscript for content, including medical writing for content; major role in the acquisition of data; analysis or interpretation of data. M.A. Rocca: drafting/revision of the manuscript for content, including medical writing for content; study concept or design; analysis or interpretation of data. M. Filippi: drafting/revision of the manuscript for content, including medical writing for content; study concept or design.

Study Funding

The authors report no targeted funding.

Disclosure

The authors declare that they have no competing interests in relation to this work. Potential conflicts of interest outside the submitted work are as follows: P. Preziosa received speaker honoraria from Roche, Biogen, Novartis, Merck, Bristol Myers Squibb, Genzyme, Horizon, and Sanofi; and has received research support from Italian Ministry of Health and Fondazione Italiana Sclerosi Multipla. E. Pagani has nothing to disclose. M. Margoni reports personal fees from Sanofi Genzyme, Merck Serono, Roche, Biogen, and Novartis. M. Rubin, L. Storelli, and G. Corazzolla have nothing to disclose. M.A. Rocca received consulting fees from Biogen, Bristol Myers Squibb, Eli Lilly, Janssen, and Roche; received speaker honoraria from AstraZaneca, Biogen, Bristol Myers Squibb, Bromatech, Celgene, Genzyme, Horizon Therapeutics Italy, Merck Serono SpA, Novartis, Roche, Sanofi, and Teva; receives research support from the MS Society of Canada, the Italian Ministry of Health, the Italian Ministry of University and Research, and Fondazione Italiana Sclerosi Multipla; and is an associate editor for *Multiple Sclerosis and Related Disorders*. M. Filippi is editor-in-chief of the *Journal of Neurology*, is an associate editor of *Human Brain Mapping*, *Neurologic Sciences*, and *Radiology*; received compensation for consulting services from Alexion, Almirall, Biogen, Merck, Novartis, Roche, and Sanofi; for speaking activities from Bayer, Biogen,

Downloaded from https://www.neurology.org by San Raffaele - MI on 11 June 2025

Celgene, Chiesi Italia SpA, Eli Lilly, Genzyme, Janssen, Merck-Serono, Neopharmed Gentili, Novartis, Novo Nordisk, Roche, Sanofi, Takeda, and TEVA; for participation in Advisory Boards for Alexion, Biogen, Bristol-Myers Squibb, Merck, Novartis, Roche, Sanofi, Sanofi-Aventis, Sanofi-Genzyme, and Takeda; and for scientific direction of educational events for Biogen, Merck, Roche, Celgene, Bristol-Myers Squibb, Lilly, Novartis, and Sanofi-Genzyme; and receives research support from Biogen Idec, Merck-Serono, Novartis, Roche, the Italian Ministry of Health, the Italian Ministry of University and Research, and Fondazione Italiana Sclerosi Multipla. Full disclosure form information provided by the authors is available with the full text of this article at Neurology.org/NN.

Publication History

Received by *Neurology® Neuroimmunology & Neuroinflammation* November 20, 2024. Accepted in final form March 26, 2025. Submitted and externally peer reviewed. The handling editor was Anne-Katrin Pröbstel, MD.

References

1. Filippi M, Bar-Or A, Piehl F, et al. Multiple sclerosis. *Nat Rev Dis Primers*. 2018;4(1):43. doi:10.1038/s41572-018-0041-4
2. Lazarevic I, Soldati S, Mapunda JA, et al. The choroid plexus acts as an immune cell reservoir and brain entry site in experimental autoimmune encephalomyelitis. *Fluids and Barriers of the CNS*. 2023;20(1):39. doi:10.1186/s12987-023-00441-4
3. Fleischer V, Gonzalez-Escamilla G, Ciolac D, et al. Translational value of choroid plexus imaging for tracking neuroinflammation in mice and humans. *Proc Natl Acad Sci U S A*. 2021;118(36):e2025000118. doi:10.1073/pnas.2025000118
4. Bergsland N, Dwyer MG, Jakimovski D, et al. Association of choroid plexus inflammation on MRI with clinical disability progression over 5 Years in patients with multiple sclerosis. *Neurology*. 2023;100(9):e911-e920. doi:10.1212/WNL.0000000000201608
5. Ricigliano VAG, Morena E, Colombi A, et al. Choroid plexus enlargement in inflammatory multiple sclerosis: 3.0-T MRI and translocator protein PET evaluation. *Radiology*. 2021;301(1):166-177. doi:10.1148/radiol.2021204426
6. Margoni M, Gueye M, Meani A, et al. Choroid plexus enlargement in paediatric multiple sclerosis: clinical relevance and effect of sex. *J Neurol Neurosurg Psychiatry*. 2023;94(3):181-188. doi:10.1136/jnnp-2022-330343
7. Preziosa P, Pagani E, Meani A, et al. Chronic active lesions and larger choroid plexus explain cognition and fatigue in multiple sclerosis. *Neurol Neuroimmunol Neuroinflamm*. 2024;11(2):e200205. doi:10.1212/NXI.0000000000200205
8. Kooij G, Kopplin K, Blasig R, et al. Disturbed function of the blood–cerebrospinal fluid barrier aggravates neuro-inflammation. *Acta neuropathologica*. 2014;128(2):267-277. doi:10.1007/s00401-013-1227-1
9. Rodríguez-Lorenzo S, Ferreira Francisco DM, Vos R, et al. Altered secretory and neuroprotective function of the choroid plexus in progressive multiple sclerosis. *Acta Neuropathol Commun*. 2020;8(1):35. doi:10.1186/s40478-020-00903-y
10. Rodríguez-Lorenzo S, Konings J, van der Pol S, et al. Inflammation of the choroid plexus in progressive multiple sclerosis: accumulation of granulocytes and T cells. *Acta Neuropathol Commun*. 2020;8(1):9. doi:10.1186/s40478-020-0885-1
11. Vercellino M, Votta B, Condello C, et al. Involvement of the choroid plexus in multiple sclerosis autoimmune inflammation: a neuropathological study. *J Neuroimmunol*. 2008;199(1-2):133-141. doi:10.1016/j.jneuroim.2008.04.035
12. Ghersi-Egea JF, Strazielle N, Catala M, Silva-Vargas V, Doetsch F, Engelhardt B. Molecular anatomy and functions of the choroidal blood-cerebrospinal fluid barrier in health and disease. *Acta Neuropathol*. 2018;135(3):337-361. doi:10.1007/s00401-018-1807-1
13. Proulx ST, Engelhardt B. Central nervous system zoning: how brain barriers establish subdivisions for CNS immune privilege and immune surveillance. *J Intern Med*. 2022;292(1):47-67. doi:10.1111/joim.13469
14. Damkier HH, Brown PD, Praetorius J. Cerebrospinal fluid secretion by the choroid plexus. *Physiol Rev*. 2013;93(4):1847-1892. doi:10.1152/physrev.00004.2013
15. Magliozzi R, Hametner S, Mastantuono M, et al. Neuropathological and cerebrospinal fluid correlates of choroid plexus inflammation in progressive multiple sclerosis. *Brain Pathol*. 2024:e13322. doi:10.1111/bpa.13322
16. Redzic ZB, Preston JE, Duncan JA, Chodobski A, Szmydynger-Chodobska J. The choroid plexus-cerebrospinal fluid system: from development to aging. *Curr Top Dev Biol*. 2005;71:1-52. doi:10.1016/S0070-2153(05)71001-2
17. Hablitz LM, Nedergaard M. The glymphatic system: a novel component of fundamental neurobiology. *J Neurosci*. 2021;41(37):7698-7711. doi:10.1523/JNEUROSCI.0619-21.2021
18. Iliff JJ, Wang M, Liao Y, et al. A paravascular pathway facilitates CSF flow through the brain parenchyma and the clearance of interstitial solutes, including amyloid β. *Sci Transl Med*. 2012;4(147):147ra111. doi:10.1126/scitranslmed.3003748
19. Taoka T, Masutani Y, Kawai H, et al. Evaluation of glymphatic system activity with the diffusion MR technique: diffusion tensor image analysis along the perivascular space (DTI-ALPS) in Alzheimer's disease cases. *Jpn J Radiol*. 2017;35(4):172-178. doi:10.1007/s11604-017-0617-z
20. Margoni M, Pagani E, Meani A, et al. Cognitive impairment is related to glymphatic system dysfunction in pediatric multiple sclerosis. *Ann Neurol*. 2024;95(6):1080-1092. doi:10.1002/ana.26911
21. Carotenuto A, Cacciaguerra L, Pagani E, Preziosa P, Filippi M, Rocca MA. Glymphatic system impairment in multiple sclerosis: relation with brain damage and disability. *Brain*. 2022;145(8):2785-2795. doi:10.1093/brain/awab454
22. Xie Y, Zhu H, Yao Y, et al. Enlarged choroid plexus in relapsing-remitting multiple sclerosis may lead to brain structural changes through the glymphatic impairment. *Mult Scler Relat Disord*. 2024;85:105550. doi:10.1016/j.msard.2024.105550
23. Li Y, Zhou Y, Zhong W, et al. Choroid plexus enlargement exacerbates white matter hyperintensity growth through glymphatic impairment. *Ann Neurol*. 2023;94(1):182-195. doi:10.1002/ana.26648
24. Xu Y, Wang M, Li X, et al. Glymphatic dysfunction mediates the influence of choroid plexus enlargement on information processing speed in patients with white matter hyperintensities. *Cereb Cortex*. 2024;34(6):bhae265. doi:10.1093/cercor/bhae265
25. Hong H, Hong L, Luo X, et al. The relationship between amyloid pathology, cerebral small vessel disease, glymphatic dysfunction, and cognition: a study based on Alzheimer's disease continuum participants. *Alzheimers Res Ther*. 2024;16(1):43. doi:10.1186/s13195-024-01407-w
26. Thompson AJ, Banwell BL, Barkhof F, et al. Diagnosis of multiple sclerosis: 2017 revisions of the McDonald criteria. *Lancet Neurol*. 2018;17(2):162-173. doi:10.1016/S1474-4422(17)30470-2
27. Valverde S, Cabezas M, Roura E, et al. Improving automated multiple sclerosis lesion segmentation with a cascaded 3D convolutional neural network approach. *Neuroimage*. 2017;155:159-168. doi:10.1016/j.neuroimage.2017.04.034
28. Storelli L, Pagani E, Rubin M, Margoni M, Filippi M, Rocca MA. A fully automatic method to segment choroid plexuses in multiple sclerosis using conventional MRI sequences. *J Magn Reson Imaging*. 2024;59(5):1643-1652. doi:10.1002/jmri.28937
29. Evans AC, Collins DL, Mills SR, Brown ED, Kelly RL, Peters TM. *3D Statistical Neuroanatomical Models from 305 MRI Volumes*. 1993 IEEE Conference Record Nuclear Science Symposium and Medical Imaging Conference, San Francisco, CA, USA. IEEE 1993; vol 3: 1813-1817
30. Balafar MA. Gaussian mixture model based segmentation methods for brain MRI images. *Artif Intelligence Rev*. 2012;41(3):429-439. doi:10.1007/s10462-012-9317-3
31. Andersson JLR, Sotiropoulos SN. An integrated approach to correction for off-resonance effects and subject movement in diffusion MR imaging. *Neuroimage*. 2016;125:1063-1078. doi:10.1016/j.neuroimage.2015.10.019
32. Basser PJ, Mattiello J, LeBihan D. MR diffusion tensor spectroscopy and imaging. *Biophys J*. 1994;66(1):259-267. doi:10.1016/S0006-3495(94)80775-1
33. Abdul-Rahman HS, Gdeisat MA, Burton DR, Lalor MJ, Lilley F, Moore CJ. Fast and robust three-dimensional best path phase unwrapping algorithm. *Appl Opt*. 2007;46(26):6623-6635. doi:10.1364/ao.46.006623
34. Sun H, Wilman AH. Background field removal using spherical mean value filtering and Tikhonov regularization. *Magn Reson Med*. 2014;71(3):1151-1157. doi:10.1002/mrm.24765
35. Alexander DC, Pierpaoli C, Basser PJ, Gee JC. Spatial transformations of diffusion tensor magnetic resonance images. *IEEE Trans Med Imaging*. 2001;20(11):1131-1139. doi:10.1109/42.963816
36. Basser PJ, Pajevic S. Statistical artifacts in diffusion tensor MRI (DT-MRI) caused by background noise. *Magn Reson Med*. 2000;44(1):41-50. doi:10.1002/1522-2594(200007)44:1<41::aid-mrm8>3.0.co;2-o
37. Jiménez AJ, Domínguez-Pinos MD, Guerra MM, Fernández-Llebrez P, Pérez-Fígares JM. Structure and function of the ependymal barrier and diseases associated with ependyma disruption. *Tissue Barriers*. 2014;2:e28426. doi:10.4161/tisb.28426
38. Choi JD, Moon Y, Kim HJ, Yim Y, Lee S, Moon WJ. Choroid plexus volume and permeability at brain MRI within the Alzheimer disease clinical spectrum. *Radiology*. 2022;304(3):635-645. doi:10.1148/radiol.212400
39. Prineas JW, Parratt JD, Kirwan PD. Fibrosis of the choroid plexus filtration membrane. *J Neuropathol Exp Neurol*. 2016;75(9):855-867. doi:10.1093/jnen/nlw061
40. Solár P, Zamani A, Kubíčková L, Dubový P, Joukal M. Choroid plexus and the blood-cerebrospinal fluid barrier in disease. *Fluids Barriers CNS*. 2020;17(1):35. doi:10.1186/s12987-020-00196-2
41. Senay O, Seethaler M, Makris N, et al. A preliminary choroid plexus volumetric study in individuals with psychosis. *Hum Brain Mapp*. 2023;44(6):2465-2478. doi:10.1002/hbm.26224
42. Zhou Y, Cai J, Zhang W, et al. Impairment of the glymphatic pathway and putative meningeal lymphatic vessels in the aging human. *Ann Neurol*. 2020;87(3):357-369. doi:10.1002/ana.25670
43. Hsu JL, Wei YC, Toh CH, et al. Magnetic resonance images implicate that glymphatic alterations mediate cognitive dysfunction in Alzheimer disease. *Ann Neurol*. 2023;93(1):164-174. doi:10.1002/ana.26516
44. Pardini M, Brown JWL, Magliozzi R, Reynolds R, Chard DT. Surface-in pathology in multiple sclerosis: a new view on pathogenesis? *Brain*. 2021;144(6):1646-1654. doi:10.1093/brain/awab025

Downloaded from https://www.neurology.org by San Raffaele - MI on 11 June 2025